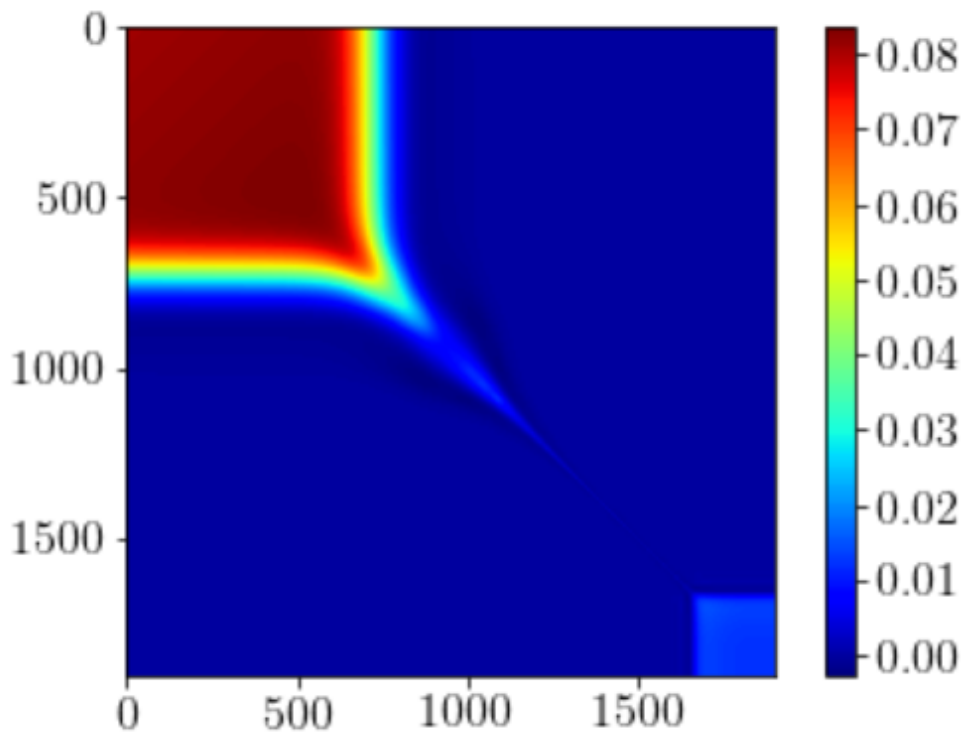
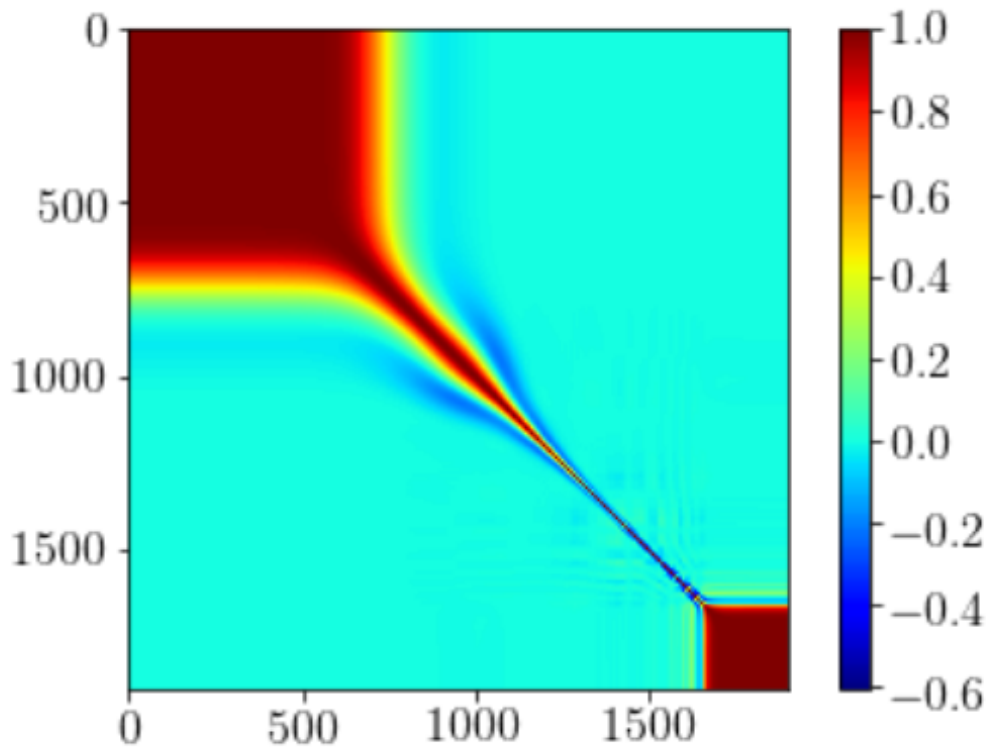


This note is to clarify the puzzling observation that the c_s reconstructions seem to have larger error bars. We were wondering where that extra error was coming from, concluding that it was due to the transfer functions that had larger support - and due to the non-diagonal covariance matrix could propagate some error from large scales to small scales.

Here is the fractional PPS covariance matrix (axes are k indices)

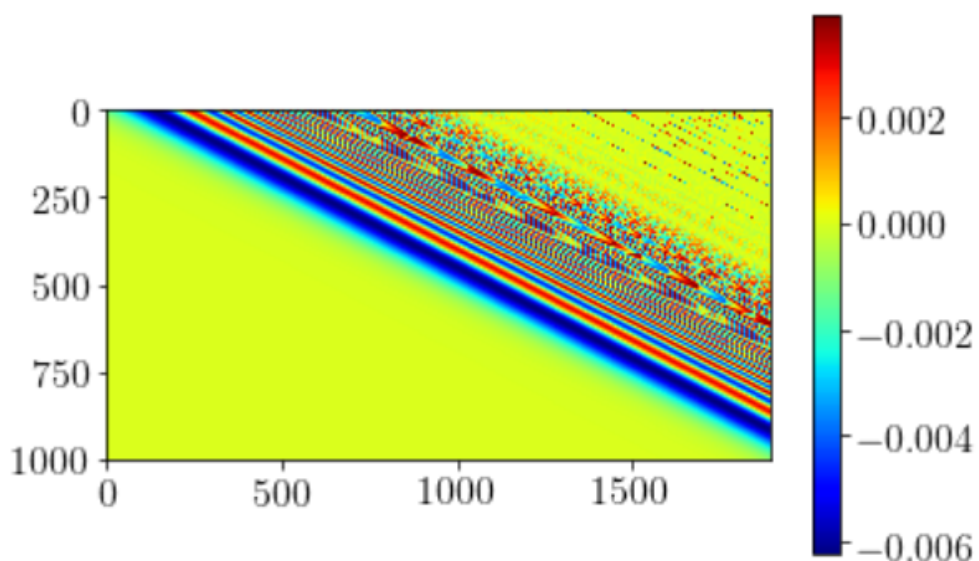


and the correlation matrix (normalised covariance matrix)

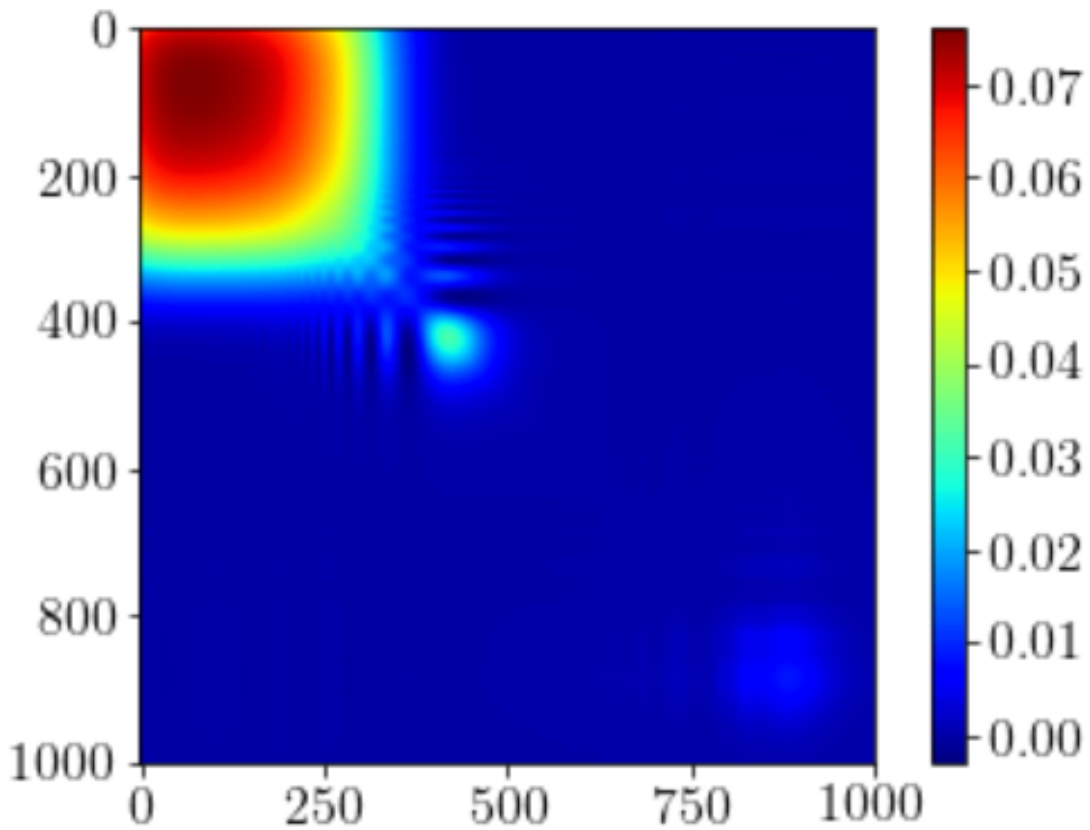


which are seen to be far from diagonal.

Since there is a linear relation between the effective PPS and the fractional change in ϵ we can transform this PPS covariance matrix to a covariance matrix of fractional changes in ϵ . This is like a basis transformation. The transfer matrix is in this case (with e-fold index along y and k index along x):



which is also seen to be non-local. The combined effect, including a Jacobian that comes from going from an effective PPS to the linear PPS, produces the fractional epsilon change covariance matrix (axes indicate the e-fold vector index)



which is also seen to depart from just having a diagonal part.

order derivatives⁹ of the PPS, as explained in detail in [31]. The Planck TT , TE and EE likelihood function consists of a pixel-based component for multipoles $\ell \leq 29$ and a Gaussian pseudo- C_ℓ component for $30 \leq \ell \leq 2508$. The fractional PPS $\Delta\mathcal{P}_\mathcal{R}/\mathcal{P}_\mathcal{R}(k)$ was then constructed by subtracting the reconstructed PPS $\mathcal{P}_\mathcal{R}(k)$ from the power-law PPS $\mathcal{P}_\mathcal{R}^{\text{pow}}(k)$ and dividing by the latter. The PPS and its uncertainty was estimated on a grid of 1900 wave numbers from $k_{\text{min}} = 6 \times 10^{-6} \text{ Mpc}^{-1}$ to $k_{\text{max}} = 0.75 \text{ Mpc}^{-1}$.

IV. RECONSTRUCTING THE INFLATON POTENTIAL

As reviewed in Appendix B, it is possible to reconstruct a potential that would reproduce an arbitrary time varying profile for ϵ assuming a canonical kinetic term for the inflaton.¹⁰ We caution that this is not the same problem as reconstructing the action for the inflaton background in general, since as discussed in §II, there will be many background models that project onto the same Wilson functions of the EFT of the adiabatic mode and thus many degeneracies exist (cf. [63–66]). Our goal here is to furnish a simple representative from the equivalence class of models that would reproduce any given profile for $\epsilon(\tau)$. From (B4), the field profile is

$$\phi(N) = \phi_0 \pm M_{\text{pl}} \int_{N_*}^N dN' \sqrt{2\epsilon(N')}, \quad (23)$$

where the choice \pm corresponds to whether we want the inflaton (and the potential it descends in) to move towards increasing or decreasing values of ϕ . The potential can correspondingly be reconstructed through (B5):

$$V(N) = V(N_*) \exp \left[-\frac{1}{3} \int_{N_*}^N dN' \left(\frac{d\epsilon}{dN'} + 6\epsilon \right) \right]. \quad (24)$$

Inverting for ϕ as a function of N and substituting into the potential above results in $V(\phi)$.

Before turning our attention towards explicit reconstructions from CMB data, we make a quick detour to discuss how one could obtain any given reconstructed PPS with a variation in the speed of sound. We note that one could just have straightforwardly inserted the expression (19) into (13) to find the reconstructed c_s^2 as a function of time, however it turns out that when one does so for both ΛCDM and EdS around an attractor for which $c_s = 1$, one necessarily requires transient phases of $c_s > 1$. One can evade this by requiring that the attractor be such that it has some constant $c_0 < 1$ (cf. [61]), in which case the relevant inversion formula is given by:

$$\frac{1}{c_s^2} - \frac{1}{c_0^2} = \frac{1}{\pi} \int_{-\infty}^0 \frac{dk}{k} \frac{\Delta_1 \mathcal{P}_\mathcal{R}}{\mathcal{P}_\mathcal{R}}(k) \sin(-2kc_0\tau). \quad (25)$$

It should not come as a surprise that there are many ways to obtain the same PPS from different choices for the functional parameters of the EFT of inflation, and the above is a manifestation of this degeneracy (see also [67–70] for a discussion of dualities between different backgrounds that produce the same PPS). An analysis of whether CMB data shows evidence for variations in the sound speed have been done within a 1st-order formalism [71, 72], and our formalism to invert for

⁹ More precisely, the penalty is proportional to $\int_0^\infty d \log k (d \log \mathcal{P}_\mathcal{R} / d \log k - (n_s - 1))^2$ where departures from a power-law $\propto k^{n_s - 1}$ with spectral index n_s are penalised.

¹⁰ It is also possible to reproduce this procedure given an *a priori* fixed non-canonical form of the kinetic term. This is one of the many model degeneracies inherent in our procedure. However, since goal of the present exercise is merely to write down a simple representative model, assuming a canonical form is sufficient for our purposes.

c_s readily applies to this case as well. However, as discussed in §II, reductions in c_s are sourced by operators that are at least two degrees higher in derivatives than those that source changes in ϵ , and so if our goal is to look for the simplest representative background models that can reproduce any given reconstructed features, it is reasonable to restrict to features induced by variations in ϵ .

V. RESULTS FOR Λ CDM

The PPS estimated from Planck Release 2 data *assuming* a Λ CDM model consistent with the best-fit Planck Release 2 parameters is shown in Fig. 5 including estimated Bayesian and frequentist uncertainties and a fiducial power-law PPS with spectral index $n_s = 0.968$. There are few indications of departures from a power-law PPS when the best-fit Λ CDM cosmological model is assumed. The most notable deviation is near $k \sim 2 \times 10^{-3} \text{ Mpc}^{-1}$ which receives dominant contributions from multipoles $\ell \sim 28$.

The reconstruction of $\epsilon(\tau)$ shown in Fig. 6 derived from this PPS is normalised such that the pivot scale $k_* = 2 \times 10^{-3} \text{ Mpc}^{-1}$ exits the horizon at $N = 0$ e-folds. An attractor background slow-roll parameter $\epsilon = 10^{-4}$ was assumed.

The reconstruction displays a prominent peak around $N \sim 3.5$ e-folds due to the $\ell \sim 28$ feature. The 1σ confidence interval on the reconstruction is given by the square root of the diagonal elements of its associated covariance matrix, obtained as described in Appendix A.

On the plot two error bands are shown, one confidence interval derived considering only the diagonal elements of the frequentist covariance matrix which describes the error in the reconstructed PPS, and the other considering the full matrix. These bands only indicate the trend in the error band as a complete analysis would require evaluating the full likelihood. In the diagonal approximation the statistical significance of a feature may appear to be high, but including the full covariance matrix increases the uncertainty in the reconstruction and lowers the significance. This is essentially because of cosmic variance on large scales which propagates to intermediate scales due to correlations between nearby wave numbers. Moreover the EFT parameters are non-local functions of the PPS, so they receive contributions from a range of wave numbers with finite support. However, it is beyond the scope of this work to present a full statistical analysis, our aim here being to demonstrate accurate EFT parameter reconstruction from a cosmological data set.

Using (B2) and (24) we obtain the potential $V(\phi)$ corresponding to the reconstructed ϵ for Λ CDM, which is shown in Fig. 7. The first thing to note is that the potential itself appears not dissimilar to that produced by a smooth polynomial. However the derivatives of the potential exhibit fine scale features, whose purpose is to knock the inflaton off the attractor solution as it evolves (right panel, Fig. 7). As expected, the derivatives of the potential closely track the reconstructed ϵ since the potential definition of the slow roll parameter $\epsilon_V \equiv M_{\text{pl}}^2 (\partial_\phi V/V)^2$ tends to the Hubble hierarchy definition $\epsilon = -\dot{H}/H^2$ when $\epsilon \ll 1$. One might reasonably ask how such effective potentials could be produced from an underlying parent theory. We shall detail various possibilities in our concluding discussion.

VI. RESULTS FOR EINSTEIN-DE SITTER

The same procedure, reconstructing the PPS from the Planck Public Release 2 data, was repeated for a cosmology *without* dark energy, the flat EdS cold+hot dark matter (CHDM) model. As shown earlier [36, 37] it requires a Hubble constant of $h \simeq 0.44$ and a 12% hot dark matter component of neutrinos with $\sum m_\nu = 2.2 \text{ eV}$. As seen in Fig. 8, large features in the reconstructed PPS are necessary for the EdS cosmology to match the data. These consist of a bump around

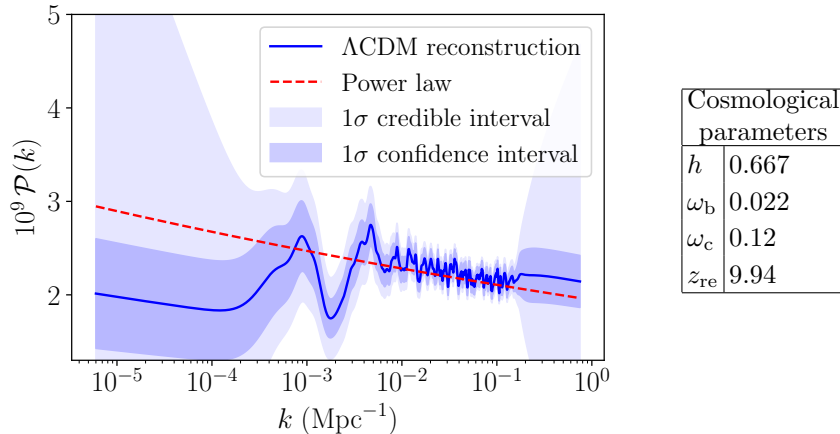


FIG. 5: Reconstruction (blue line) of the PPS from Planck Public Release 2 TT , TE and EE data assuming a Λ CDM cosmological model with cosmological parameters listed in the table (right). The purple band indicates the 1σ confidence interval and the light blue band indicates the 1σ credible interval. A power-law PPS (red dashed line) with $n_s = 0.968$ is superimposed.

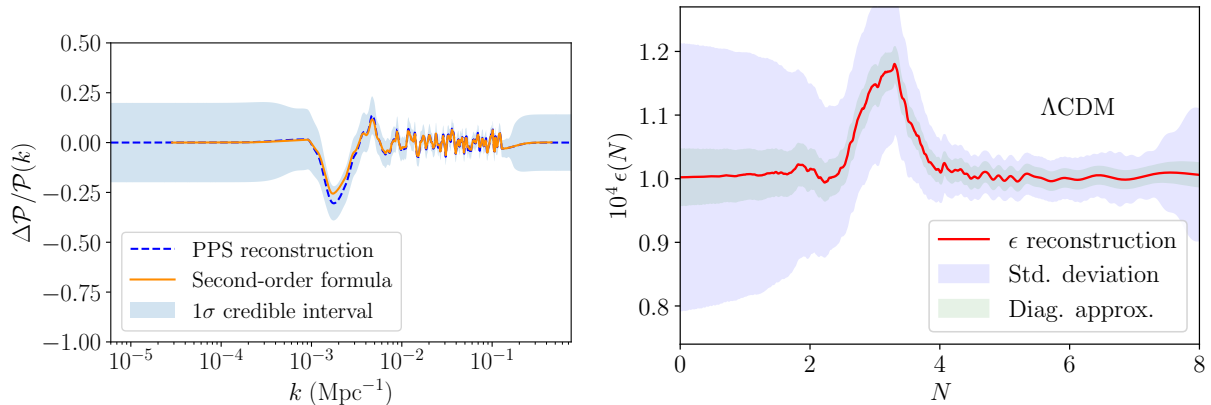


FIG. 6: The right panel shows the 2nd-order reconstructed ϵ for the $\Delta\mathcal{P}_R/\mathcal{P}_R$ estimated from Planck data assuming Λ CDM (left panel, dashed blue line). The blue (full covariance matrix) and green (its diagonal approximation) shaded bands indicate the 1σ uncertainties in ϵ due to errors in the estimated PPS. The orange line in the left panel is the PPS obtained by numerical integration of the reconstructed ϵ .

$k \sim 2 \times 10^{-2} \text{ Mpc}^{-1}$ followed by oscillations that continue until $k \sim 2 \times 10^{-1} \text{ Mpc}^{-1}$. These oscillations ensure that the model fits the small scale CMB acoustic peaks. A model involving two successive phase transitions during multiple inflation which reproduces the general shape of the reconstructed PPS had been proposed in [36, 37], however it admittedly does not yield the oscillatory small-scale fine structure.

The EdS $\epsilon(\tau)$ estimate of Fig. 10 again exhibits a large peak at $N \sim 3.5$ but now also features seemingly sharp oscillations at $N \sim 5$ corresponding to the small scale oscillations in the PPS. Repeating the same error analysis as was done for the Λ CDM case, the error in the reconstructed EFT parameter due to the uncertainty in the estimated PPS was obtained. Both the full and diagonal contributions of the PPS covariance matrix to the standard deviation of ϵ were again

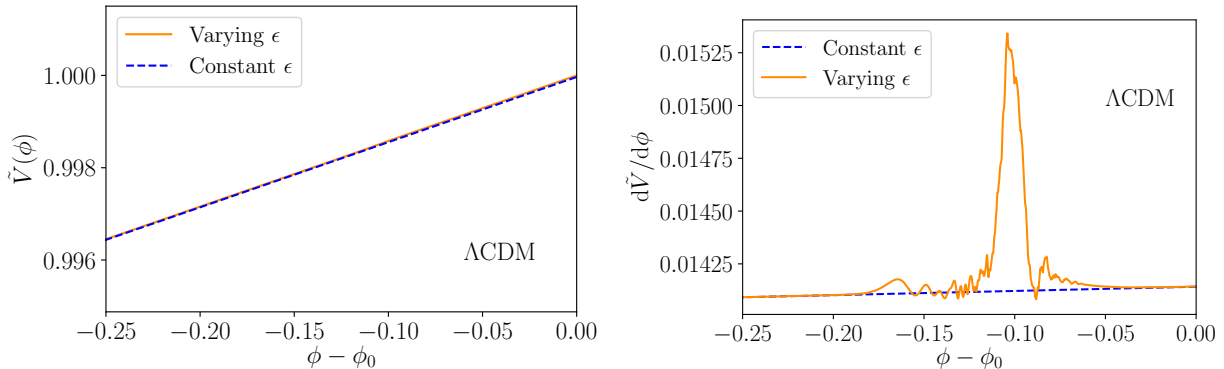


FIG. 7: The left panel shows the potential $\tilde{V} = V(\phi)/V(\phi_0)$ corresponding to the reconstructed $\Delta\epsilon/\epsilon$ superposed on the attractor potential (dashed blue line) – the right panel is its derivative.

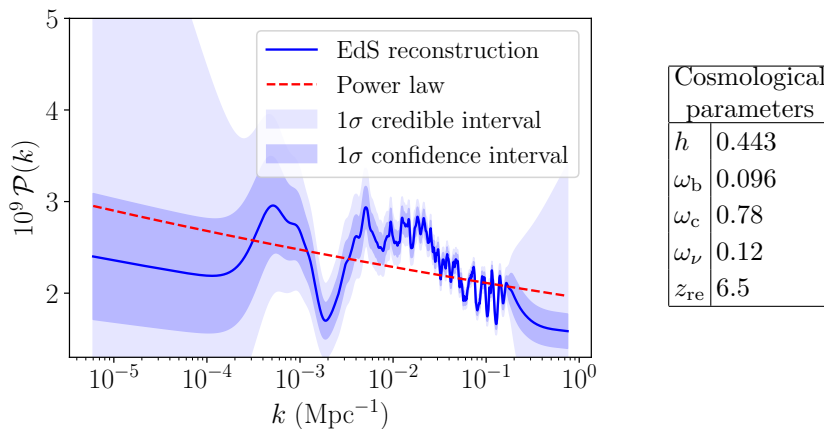


FIG. 8: The estimated PPS for the EdS cosmological model with neutrino dark matter from Planck Release 2 TT , TE and EE data. The left panel shows the reconstructed PPS (blue line) with credible (purple band) and confidence intervals (light blue band) with $n_s = 0.968$ power-law PPS (red dashed line) superimposed. The right panel shows the cosmological parameters.

considered. It is seen that the off-diagonal elements make a large contribution to the uncertainty in ϵ and lower the statistical significance of the features. However the sharp feature at $N \sim 5$ is still required when an EdS cosmology is assumed.

Although this may seem like a sudden change in an EFT parameter over < 1 e-fold, the degree of suddenness is quantified by the second term in the Hubble hierarchy $\eta \equiv \dot{\epsilon}/\epsilon H$, which is bounded throughout by $|\eta| \lesssim 1.5$, leaving us safely within the single clock regime [73] (also true for the Λ CDM case (Fig. 7)). As in the previous section, one can reconstruct the potential that could have given rise to the reconstructed feature that best fits an underlying EdS cosmology (cf. Fig. 9). We see again that the potential itself looks similar to a smooth polynomial over the field excursion needed to produce the observed modes. However, its derivatives vary along the trajectory tracking ϵ closely in just such a manner as to knock the background off the attractor, producing the required features. This occurs in a manner that produces a fit to the reconstructed PPS accurate to the percent level *without* needing to invoke any phase transitions (as in [36, 37]). It remains for us to elaborate on the nature of the parent theory that could have produced such an effective potential.

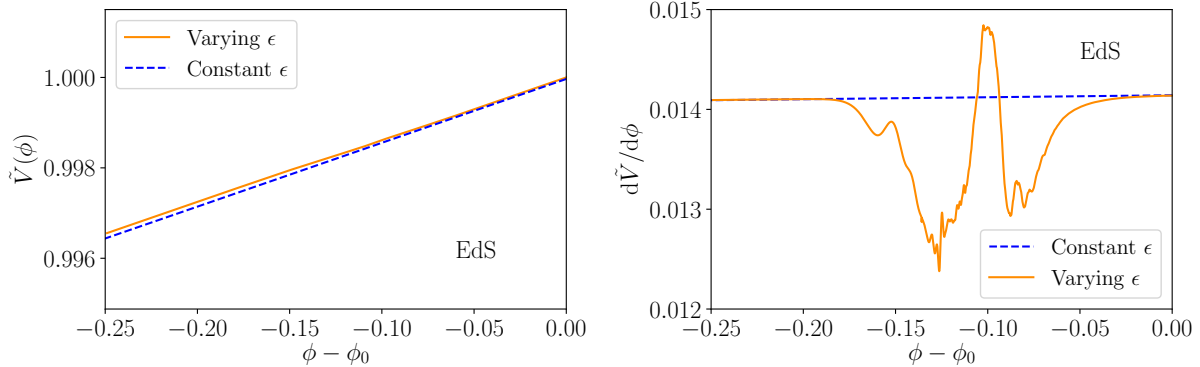


FIG. 9: The left panel shows the potential $\tilde{V} = V(\phi)/V(\phi_0)$ corresponding to $\Delta\epsilon/\epsilon$ superposed on the attractor potential (dashed blue line), and its derivative (right panel).

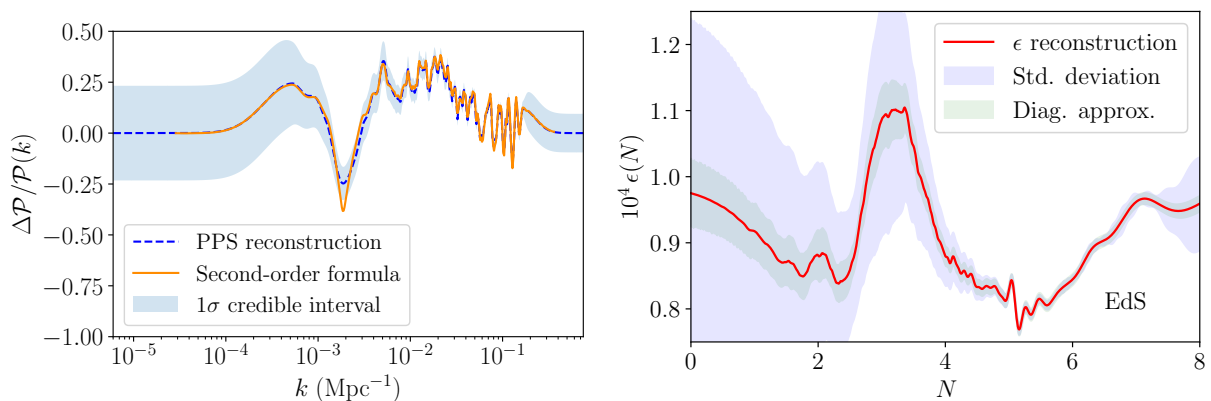


FIG. 10: The right panel shows the 2nd-order reconstructed ϵ for the $\Delta\mathcal{P}_{\mathcal{R}}/\mathcal{P}_{\mathcal{R}}$ (left panel, dashed blue line) estimated from Planck data assuming the EdS cosmological model. The green (diagonal approximation) and blue (full matrix) bands indicate the 1σ uncertainties in ϵ due to errors in the estimated PPS. The orange line is the result of numerical integration of the power spectrum given the reconstructed ϵ .

VII. DISCUSSION

Having seen how to reconstruct potentials that can produce any given power spectrum, one might wonder how such effective potentials might arise in realistic settings. Viewing the effective action for the inflaton background as having been obtained by integrating out all heavy degrees of freedom in the parent theory, one can for example obtain leading order (adiabatic) corrections to the inflaton potential of the form (cf. (C4) and (C12))

$$\partial_\phi V_{\text{CW}}(\phi) = \frac{\partial_\phi M^2(\phi)}{32\pi^2} M^2(\phi) \ln[M^2(\phi)/\mu^2], \quad (26)$$

where the above was obtained by integrating out a heavy field with an effective mass given by $M^2(\phi)$ that is taken to vary weakly enough with respect to ϕ i.e.

$$\dot{\phi}_0 \partial_\phi M/M^2 \ll 1 \quad (27)$$

where ϕ_0 denotes the background trajectory, and where the inflaton effective potential is given by the sum of the above correction plus the background field contribution $V_{\text{eff}} = V_{\text{inf}} + V_{\text{CW}}$ (cf. eq.C4). Violating (27) necessarily implies particle production resulting from higher orders in the adiabatic expansion that one can calculate (reviewed in Appendix C). Indeed, the possibility of localised particle production events along the inflaton trajectory was considered in [74–78] and can generate additional features in the effective potential. However one has to study these cases more carefully given the possibility of production and subsequent decay of isocurvature modes – removing us from the single clock context upon which this study relies. One can nevertheless quantify the requirement of staying within the adiabatic approximation in generating the features in the effective potential required to produce the finer features, such as in the EdS case (cf. Fig. 10). Re-expressing (27) as

$$\sqrt{2\epsilon} \frac{H}{M} \frac{\partial}{\partial \tilde{\phi}} \log M = \sqrt{\frac{\epsilon}{8}} \frac{H}{M} \frac{\partial}{\partial \tilde{\phi}} \log V_{\text{CW}} \ll 1 \quad (28)$$

where the partial derivative is with respect to $\tilde{\phi} = \phi/M_{\text{pl}}$, we find that the logarithmic derivative of the potential around the finer feature in Fig. 9 to be order unity. Given the value of ϵ around the fiducial attractor presented in the plot is $\epsilon_0 = 10^{-4}$, and given the assumption that the mass of the heavy field is much greater than Hubble, the condition (28) is readily satisfied.

We stress that the formalism developed here allows one to obtain the parameters of the EFT of inflation given any particular set of assumptions for the reconstruction. The examples presented here were of reconstructions presuming a background Λ CDM or Einstein-de Sitter cosmology with a fixed set of parameters, but are equally applicable to other examples.¹¹ One can thus ‘invert’ for background models that could reproduce any given reconstructed primordial power spectrum provided $(\Delta\mathcal{P}_{\mathcal{R}}/\mathcal{P}_{\mathcal{R}})^3$ is less than the 1σ confidence interval of the reconstruction $\Sigma(k)$.

Acknowledgements

We would like to thank Ana Achucarro and Gonzalo Palma for helpful discussions and the Referee for a helpful query which led us to critically reexamine the error bands on our reconstructed parameters. The authors were supported by a Niels Bohr Professorship award to SS by the Danmarks Grundforskningsfond.

Appendix A: Feature inversion

We recall the leading order action (8):

$$S_2 = M_{\text{pl}}^2 \int d^4x a^3 \epsilon \left(\frac{\dot{\mathcal{R}}^2}{c_s^2} - \frac{(\partial\mathcal{R})^2}{a^2} \right). \quad (A1)$$

We imagine the background of interest (characterised by $c_s(\tau)$ and $\epsilon(\tau)$) is a small perturbation about a fiducial attractor solution with constant ϵ and $c_s = 1$, to which it tends at early and late times. The small quantities $\Delta\epsilon/\epsilon(\tau)$ and $u(\tau) = 1/c_s(\tau) - 1$ then define a perturbative expansion. We use the in-in formalism to calculate the fractional change in the power spectrum at 1st- and

¹¹ For instance, one can consider the possibility that discrepancy between low redshift measurements of H_0 and those obtained from CMB observations can be projected onto a primordial power spectrum with specific features [79].

- from Multiple-Field Curved Valleys,” JHEP **1301**, 133 (2013) [arXiv:1209.5701 [hep-th]].
- [58] A. Achucarro, J. O. Gong, S. Hardeman, G. A. Palma and S. P. Patil, “Effective theories of single field inflation when heavy fields matter,” JHEP **1205**, 066 (2012) [arXiv:1201.6342 [hep-th]].
- [59] A. Achucarro, J. O. Gong, S. Hardeman, G. A. Palma and S. P. Patil, “Mass hierarchies and non-decoupling in multi-scalar field dynamics,” Phys. Rev. D **84**, 043502 (2011) [arXiv:1005.3848 [hep-th]].
- [60] A. Achucarro, J. O. Gong, S. Hardeman, G. A. Palma and S. P. Patil, “Features of heavy physics in the CMB power spectrum,” JCAP **1101**, 030 (2011) [arXiv:1010.3693 [hep-ph]].
- [61] S. Cespedes, V. Atal and G. A. Palma, “On the importance of heavy fields during inflation,” JCAP **1205**, 008 (2012) [arXiv:1201.4848 [hep-th]].
- [62] A. Achucarro, V. Atal, S. Cespedes, J. O. Gong, G. A. Palma and S. P. Patil, “Heavy fields, reduced speeds of sound and decoupling during inflation,” Phys. Rev. D **86**, 121301 (2012) [arXiv:1205.0710 [hep-th]].
- [63] K. Kadota, S. Dodelson, W. Hu and E. D. Stewart, “Precision of inflaton potential reconstruction from CMB using the general slow-roll approximation,” Phys. Rev. D **72**, 023510 (2005) [astro-ph/0505158].
- [64] J. M. Cline and L. Hoi, “Inflationary potential reconstruction for a wmap running power spectrum,” JCAP **0606**, 007 (2006) [astro-ph/0603403].
- [65] R. Bean, D. J. H. Chung and G. Geshnizjani, “Reconstructing a general inflationary action,” Phys. Rev. D **78**, 023517 (2008) [arXiv:0801.0742 [astro-ph]].
- [66] C. S. Gauthier and R. Akhoury, “Reconstructing Single Field Inflationary Actions From CMBR Data,” JCAP **0807**, 022 (2008) [arXiv:0804.0420 [astro-ph]].
- [67] D. Wands, “Duality invariance of cosmological perturbation spectra,” Phys. Rev. D **60**, 023507 (1999) [gr-qc/9809062].
- [68] D. Baumann, L. Senatore and M. Zaldarriaga, “Scale-Invariance and the Strong Coupling Problem,” JCAP **1105**, 004 (2011) [arXiv:1101.3320 [hep-th]].
- [69] A. Joyce and J. Khoury, “Strong Coupling Problem with Time-Varying Sound Speed,” Phys. Rev. D **84**, 083514 (2011) [arXiv:1107.3550 [hep-th]].
- [70] A. Gallego Cadavid and A. E. Romano, “One spectrum to rule them all?,” Phys. Lett. B **793**, 1 (2019) [arXiv:1712.00089 [astro-ph.CO]].
- [71] A. Achucarro, V. Atal, B. Hu, P. Ortiz and J. Torrado, “Inflation with moderately sharp features in the speed of sound: Generalized slow roll and in-in formalism for power spectrum and bispectrum,” Phys. Rev. D **90**, no. 2, 023511 (2014) [arXiv:1404.7522 [astro-ph.CO]].
- [72] J. Torrado, B. Hu and A. Achucarro, “Robust predictions for an oscillatory bispectrum in Planck 2015 data from transient reductions in the speed of sound of the inflaton,” Phys. Rev. D **96**, no. 8, 083515 (2017) [arXiv:1611.10350 [astro-ph.CO]].
- [73] C. T. Byrnes, P. S. Cole and S. P. Patil, “Steepest growth of the power spectrum and primordial black holes,” arXiv:1811.11158 [astro-ph.CO].
- [74] M. A. Amin and D. Baumann, “From Wires to Cosmology,” JCAP **1602**, no. 02, 045 (2016) [arXiv:1512.02637 [astro-ph.CO]].
- [75] M. A. Amin, M. A. G. Garcia, H. Y. Xie and O. Wen, “Multifield Stochastic Particle Production: Beyond a Maximum Entropy Ansatz,” JCAP **1709**, no. 09, 015 (2017) [arXiv:1706.02319 [astro-ph.CO]].
- [76] M. A. G. Garcia, M. A. Amin, S. G. Carlsten and D. Green, “Stochastic Particle Production in a de Sitter Background,” JCAP **1905**, no. 05, 012 (2019) [arXiv:1902.09598 [astro-ph.CO]].
- [77] S. Choudhury, A. Mukherjee, P. Chauhan and S. Bhattacharjee, “Quantum Out-of-Equilibrium Cosmology,” arXiv:1809.02732 [hep-th].
- [78] S. Choudhury and A. Mukherjee, “Quantum randomness in the Sky,” arXiv:1812.04107[physics.gen-ph]
- [79] D. K. Hazra, A. Shafieloo and T. Souradeep, “Parameter discordance in Planck CMB and low-redshift measurements: projection in the primordial power spectrum,” arXiv:1810.08101 [astro-ph.CO].
- [80] A. Durakovic, Ph.D thesis, University of Copenhagen 2018.
- [81] P. Adshead, R. Easther and E. A. Lim, “The ‘in-in’ Formalism and Cosmological Perturbations,” Phys. Rev. D **80**, 083521 (2009) doi:10.1103/PhysRevD.80.083521 [arXiv:0904.4207 [hep-th]].
- [82] S. R. Coleman and E. J. Weinberg, “Radiative Corrections as the Origin of Spontaneous Symmetry Breaking,” Phys. Rev. D **7**, 1888 (1973).
- [83] H. E. Kandrup, “Particle Number and Random Phases,” Phys. Rev. D **38**, 1773 (1988).
- [84] H. E. Kandrup, “Stochastic Inflation As A Time Dependent Random Walk,” Phys. Rev. D **39**, 2245 (1989).